Emergence of quasiperiodic regimes in a neutral delay model of flute-like instruments: Influence of the detuning between resonance frequencies

Soizic Terrien, Christophe Vergez, Benoît Fabre, Patricio de la Cuadra

Emergence of quasiperiodic regimes in a neutral delay model of flute-like instruments: influence of the detuning between resonance frequencies

Soizic Terrien*

Laboratoire d'Acoustique de l'Université du Mans (LAUM), UMR 6613,
Institut d'Acoustique - Graduate School (IA-GS), CNRS, Le Mans Université,
Le Mans, France

Christophe Vergez

Aix Marseille Univ, CNRS, Centrale Marseille, LMA UMR7031,
Marseille, France

Benoît Fabre

Sorbonne Université, CNRS, Institut Jean Le Rond d'Alembert, UMR 7190,
Paris, France

Patricio de la Cuadra

Escuela de Ingeniería-Instituto de Música, Pontificia Universidad Católica de Chile,
Santiago, Chile

(Communicated by the associate editor name)

Abstract

Musical instruments display a wealth of dynamics, from equilibria (where no sound is produced) to a wide diversity of periodic and non-periodic sound regimes. We focus here on two types of flute-like instruments, namely a recorder and a pre-hispanic Chilean flute. A recent experimental study showed that they both produce quasiperiodic sound regimes which are avoided or played on purpose depending on the instrument. We investigate the generic model of sound production in flute-like musical instruments, a system of neutral delay-differential equations. Using time-domain simulations, we show that it produces stable quasiperiodic oscillations in good agreement with experimental observations. A numerical bifurcation analysis is performed, where both the delay time (related to a control parameter) and the detuning between the resonance frequencies of the instrument – a key parameter for instrument makers – are considered as bifurcation parameters. This demonstrates that the large detuning that is characteristic of prehispanic Chilean flutes plays a crucial role in the emergence of stable quasiperiodic oscillations.

1 Introduction

Self-sustained musical instruments (brass, woodwind and bowed strings) have attracted considerable attention from physicists and dynamicists for decades. They exhibit a wealth of dynamics, from equilibrium regimes where no sound is produced despite an action of the musician to periodic regimes, quasiperiodic modulated sounds and chaotic oscillations [1, 38, 39]. This wide diversity results from complex sound production mechanisms involving different fields of physics, from contact mechanics to hydrodynamics or fluid-structure interaction, many of whom remain only partially understood. The

acoustical features of the different sound regimes depend sensitively on both the control parameters adjusted by the musician and the intrinsic parameters determined when the instrument is made (such as the geometry and constitutive material) [31, 35, 34].

We focus here on flute-like instruments, which include a wide variety of instruments such as ocarina, recorders, transverse flutes and many other instruments from different cultures and countries. In all these instruments, sound production relies on the nonlinear coupling between a naturally unstable air jet blown by the musician and an acoustic field contained in the instrument pipe [4]. We focus more particularly on the emergence of non-periodic sound regimes in a recorder and in a pre-hispanic Chilean flute. A recent experimental study showed that both these instruments produce stable quasiperiodic regimes [16]. The corresponding sounds are provided as supplementary material of [16] and the recorded time series are reproduced in Figure 1. In the case of the recorder, such sounds are usually avoided and considered as a defect of the instrument or as a lack of control from the musician. Periodic regimes are on the contrary the typical regimes produced by the musician, as they correspond to the different notes of the musical scale. On the other hand, in the pre-hispanic Chilean flute, quasiperiodic regimes are played on purpose to produce specific sound effects and correspond to the regular playing mode [28, 15, 16]. In this article, we investigate the emergence of such quasiperiodic sound regimes, in relation to a delay time τ which is related to the musician's blowing pressure. We also investigate the role played by the detuning between the resonance frequencies. This intrinsic parameter related to the internal geometry of the instrument is often referred to as inharmonicity (see for example [34]). It is defined as the relative difference between the n^{th} resonance frequency and the n^{th} resonance frequency of an ideal, perfectly cylindrical resonator without losses. The latter is equal to the n^{th} or $(2n+1)^{th}$ integer multiple of the first resonance frequency, depending, respectively, whether the resonator is open on both ends or has one close end and one open end [3]. The important role of inharmonicity on the properties of sound regimes is well identified by instrument makers, and has been highlighted qualitatively in other families of musical instruments [33, 34, 43]. However, its quantitative effects on the stability of periodic regimes and on the emergence of quasiperiodic regimes as well as the difference between the effect of a positive and a negative inharmonicity remain open questions, in particular in the case of flute-like instruments. Because some level of inharmonicity is unavoidable in practice, these are important question in the context of instrument making. In instruments with side toneholes (such as recorders and transverse flutes but also clarinets and saxophones), although the acoustical response of the resonator changes drastically depending on the considered fingering (*i.e.* the combination of open and closed toneholes as chosen by the musician), a single physical resonator with a given geometry is used to play all the notes of the instrument. In comparison with pan-like flutes or organs, where one resonator is used for each note, controlling the level of inharmonicity for all the different fingerings is a much more challenging task for the instrument maker. In contrast to recorders, the regular playing mode of prehispanic Chilean flutes considered here corresponds to quasiperiodic regimes. Another peculiarity of theses instruments lies in the shape of the resonator which is made of two cylinders of similar length but different ratio (as represented schematically Figure 2). This has been shown to favor a strong inharmonicity [15]. Here we investigate the influence of inharmonicity on the emergence of stable quasiperiodic oscillations in both recorders and prehispanic Chilean flutes. Because they correspond either to the regular playing mode or to a defect of the instruments, understanding how to favor or to avoid quasiperiodic sound regimes is particularly valuable in the context of instrument making.

We consider the jet-drive model, a generic model of flute-like instruments written in the form of neutral delay-differential equations (NDDEs). This model has been studied by means of a one-parameter numerical bifurcation analysis only recently [20]. In the classical case of a recorder or transverse flute, it has shown excellent agreement with the most common bifurcation scenario observed in an actual experiment when the musician's mouth pressure is increased. In such a case, successive jumps between periodic regimes with increasing frequencies (corresponding to notes of the musical scale) are observed, with no non-periodic sound regimes [31, 32, 20].

Delay differential equations (DDEs) have an infinite-dimensional phase space [40, 41], and specific numerical methods have to be used for their time-domain simulation and continuation [44]. In particular, in contrast to ordinary differential equations (ODEs) where initial conditions are defined only at

$t = 0$, solving delay differential equations (DDEs) requires to specify the history on a whole internal $[-\tau, 0]$. Compared to DDEs, NDDEs contain derivatives of delayed terms and can display more complicated bifurcation scenarios and dynamics [37]. The simulation, numerical continuation and bifurcation analysis of NDDEs implies to use dedicated advanced numerical methods. In this paper, time-domain simulations are performed using the Matlab solver ddensd [42]. Numerical continuation and bifurcation analysis are performed in the Matlab-based continuation software DDE-Biftool [24, 23, 25], in which the collocations schemes for neutral systems described in [26, 27] have been implemented [20].

The model is described in more details in section 2, and the main parameters are recalled. The geometrical details of the two instruments considered here are taken into account through their acoustic input admittance. In section 3, we use numerical simulations to investigate the ability of the generic model to reproduce the quasiperiodic regimes, including their specific acoustical features, observed experimentally in the recorder and in the pre-hispanic Chilean flute, [16]. Simulated sounds are analysed in the Fourier domain and in the phase space. This reveals that the generic model can produce quasiperiodic sounds that share many properties with sounds produced by real instruments. In section 4, we perform a numerical bifurcation analysis where both the delay τ and the inharmonicity (detuning between resonance frequencies) are considered as bifurcation parameters. This highlights the key role played by the detuning parameter in the emergence of stable quasiperiodic regimes.

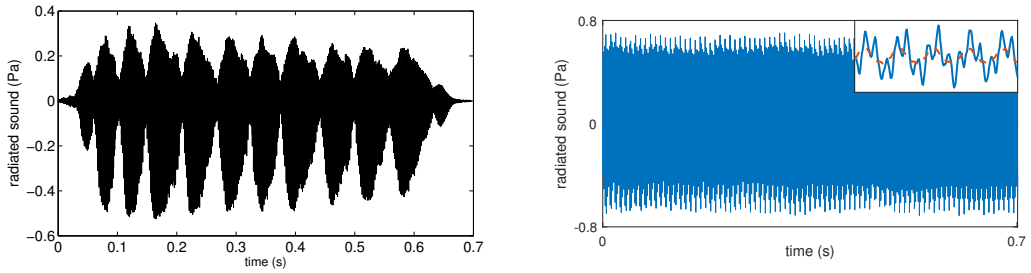

Figure 1: Radiated sound produced by a Chilean flute (left) played by an experienced player, and by an alto recorder (right) played by a pressure-controlled artificial mouth. The blowing pressure is around 1260 Pa for the Chilean flute and fixed to 650 Pa for the recorder. The inset shows an enlargement on the first 0.01 seconds of the signal (solid blue line), and displays a comparison with the waveform of the periodic sound (dashed red line) obtained using the same instrument and same fingering, but for a lower blowing pressure $P_m = 350$Pa. The corresponding sounds are available online as supplementary material of [16].

2 Physical model of flute-like musical instruments

Musical instruments such as organs, flutes, reed (clarinet, oboe, ...), brass (trumpet, trombone) and bowed-string instruments (violin, cello ...) are self-sustained oscillators. They are classically described by a coupled system consisting of a nonlinear exciter and a linear, passive acoustic resonator [1].

2.1 Exciter

A fundamental difference between flute-like instruments and other blowing (wind) instruments lies in the nature of the exciter [2]. In reed and brass instruments, the excitation mechanism relies on the vibration of a solid element (a cane reed or the lips of the musician, respectively) [3]. Flute-like instruments, on the contrary, are essentially fluid oscillators: the exciter consists of a naturally unstable air jet interacting with a sharp edge of the instrument, referred to as the *labium*. Figure 3 shows a schematic representation of a recorder. Considering this instrument as an example, the mechanism of

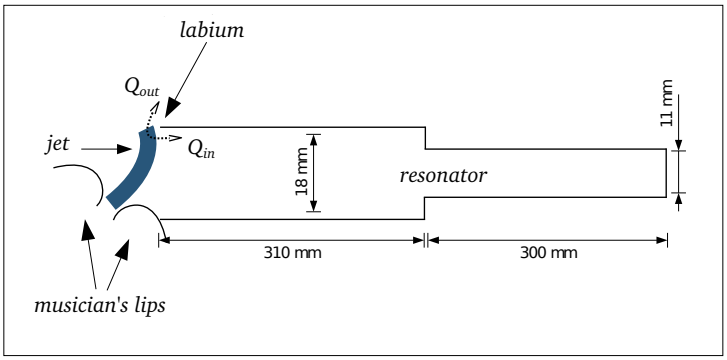

Figure 2: Schematic representation of a Chilean flute, highlighting the shape of the resonator. The air jet oscillating around the labium is represented in blue. Q_{in} and Q_{out} represent the alternate flow injection inside and outside of the resonator, which constitutes the source.

sound production can be described as follows [4]. When the musician blows into the channel of the instrument, an air jet with a Bickley profile in created at the channel exit [5]. The central velocity U_j of the air jet is linked to the pressure difference between the musician's mouth cavity and the atmosphere through Bernoulli's law, and its semi-half width b is estimated as $2h/5$ with h the channel height at its exit [6]. Because the air jet is naturally unstable [7], any small perturbation is amplified and convected along the jet, across the window of length W (see Figure 3). The spatial amplification rate α_i and convection velocity c_p have been estimated experimentally as $\alpha_i \approx 0.4/h$ and $c_p \approx 0.4U_j$, respectively [8, 9, 5]. The jet-labium interaction leads to the oscillation of the jet around the labium, with a transversal deflection $\eta(t)$ of the jet centerline. This oscillation results in an alternate flow injection outside and inside the instrument. These two flow sources are referred to as Q_{out} and Q_{in}, respectively, and are separated from each other by a small distance δ_d, evaluated by Verge as $\delta_d = \frac{4}{\pi}\sqrt{2hW}$ [10]. Overall, they act as a dipolar source of pressure $p(t)$ which excites the acoustic resonator composed of the air column contained in the instrument pipe. The resonator acts as a filter which favors or inhibits certain frequency components in the spectrum of the acoustic field. Finally, the acoustic waves in the resonator perturb back the unstable air jet at the channel exit [11, 9]. These perturbations are amplified while being convected along the air jet, thus sustaining the oscillation of the jet around the labium and, as such, the sound production. The convection time of this perturbation along the jet introduces a delay time $\tau = W/c_p$. Importantly, the value of τ is directly related to the pressure in the musician's mouth and is, as such, the main control parameter.

Although the physics behind the sound production is similar in both instruments considered in this article, it is worth noting that the exciter part of the two instrument significantly differ from each other. For the recorder, most geometrical parameters are fixed by the instrument maker (see Figure 3). For the Chilean flute on the other hand, the channel is not a part of the instrument but is rather formed by the musician lips, and the labium is one of the instrument edges, as shown in Figure 2. Many of the exciter parameters are then directly controlled by the musician: this includes the length W of the jet, the height h of the channel and the offset y_0 between the channel centerline and the labium. Because these parameters can change significantly during the musical performance, their estimation is more complicated.

2.2 Resonator

The response of the resonator to the excitation by the source of pressure is described in the frequency domain, through its input acoustic admittance $Y(\omega)$. This approach allows to take into account the

influence of the complex inner shape of the instruments. The admittance is defined as the ratio, in the frequency domain, between the acoustic velocity below the labium $V_{ac}(\omega)$ and the source of pressure $P(\omega)$ resulting from the interaction between the air jet and the labium:

$$Y(\omega) = \frac{V_{ac}(\omega)}{P(\omega)}. \tag{1}$$

It can be either measured experimentally [12, 13] or determined from analytical formulae [3], and is commonly represented in the Fourier domain as a sum of an infinite number of resonance modes [3]:

$$Y(\omega) = \sum_{n=1}^{\infty} \frac{a_n i\omega}{\omega_n^2 - \omega^2 + i\omega\frac{\omega_n}{Q_n}}, \tag{2}$$

with ω the angular frequency and a_n, ω_n and Q_n the amplitude, resonance angular frequency, and quality factor of the n^{th} resonance mode, respectively. Here, this sum is truncated to take into account the first five modes [14], whose resonance frequencies span the frequency band of interest in the musical context.

The resonators of the two instruments considered in this article are significantly different from each other [16]. The resonator of the recorder can be represented, in first approximation, as a cylinder open on both ends. By closing or opening the different tonholes along the resonator, the musician can change the resonator properties (and in particular its apparent length), and thus access a wealth of sound regimes. On the other hand, the resonator of Chilean flutes is composed of two cylinders in series, with similar length but with diameters in a ratio close to two [15] (see Figure 2). Similarly to Pan flutes, it has one open end on the musician's side, one closed end, and no toneholes.

The input admittance of the recorder is calculated using the software WIAT [18], from the precise knowledge of its inner geometry [19]. On the other hand, an experimentally measured admittance is considered for the Chilean flute [16]. In both cases, the modal parameters in equation (2) are estimated using an optimisation procedure (least square method). Figure 4 shows, for both instruments, the comparison between the original (calculated or measured) admittance and the fitted admittance represented as a sum of five resonance modes. The corresponding modal parameters are given in Table 1. Because the recorder has an open-open resonator, a sixth mode has to be taken into account to ensure the convergence at zero frequency. It is written in a slightly different form [3, 20]:

$$Y_0(\omega) = \frac{a_0}{i\omega b_0 + c_0}. \tag{3}$$

Overall, Figure 4 shows excellent agreement between the original and fitted admittances, in particular around the resonance frequencies (i.e. around the maxima of $|Y(\omega)|$). For the Chilean flute, the differences are more important around anti-resonances (minima of $|Y(\omega)|$). This is due to the fact that only a finite number of resonance modes is taken into account. However, the instrument playing frequencies are close to the resonance frequencies [31], and we therefore expect these differences to have little effect on the observed dynamics. Finally, the resonator is described by the following equation:

$$V_{ac}(\omega) = \left(\frac{a_0}{i\omega b_0 + c_0} + \sum_{n=1}^{5} \frac{a_n i\omega}{\omega_n^2 - \omega^2 + i\omega\frac{\omega_n}{Q_n}} \right) P(\omega), \tag{4}$$

with $a_0 = 0$ for the Chilean flute, as explained above. From equation (4), $V_{ac}(\omega)$ is written as the sum of the contribution of the different resonance modes:

$$V_{ac}(\omega) = V_{ac0}(\omega) + \sum_{n=1}^{5} V_{acn}(\omega), \tag{5}$$

where:

$$\begin{aligned} V_{ac0}(\omega) &= \frac{a_0}{i\omega b_0 + c_0} P(\omega), \\ V_{acn}(\omega) &= \frac{a_n i\omega}{\omega_n^2 - \omega^2 + i\omega\frac{\omega_n}{Q_n}} P(\omega). \end{aligned} \tag{6}$$

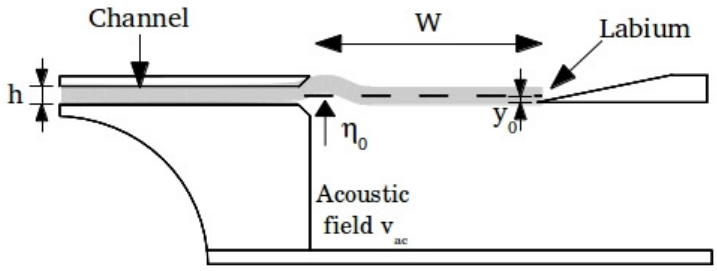

Figure 3: Schematic representation of the cross section of the upper part of a recorder flute. The naturally unstable air jet blown by the musician is perturbed by the internal acoustic field v_{ac} at the channel exit, leading to a transversal deflection η_0 of the jet. This perturbation is subsequently convected and amplified along the jet.

Using equations (6), equations (4) and (5) are written in the time-domain through an inverse Fourier transform, which leads to:

$$\begin{aligned} v_{ac}(t) &= v_{ac0}(t) + \sum_{n=1}^{5} v_{acn}(t), \\ \dot{v}_{ac0}(t) &= \frac{a_0}{b_0} p(t) - \frac{c_0}{b_0} v_{ac0}(t), \\ \ddot{v}_{acn}(t) &= a_n \dot{p}(t) - \omega_n^2 v_{acn}(t) - \frac{\omega_n}{Q_n} \dot{v}_{acn}(t), \quad \forall n \in [1,5]. \end{aligned} \tag{7}$$

2.3 A system of neutral delay-differential equations

Overall, the state-of-the art model of flute-like instruments is formed by system (7) together with the following equations:

$$\begin{aligned} \eta(t) &= \frac{h}{U_j} e^{\alpha_i W} v_{ac}(t-\tau), \\ p(t) &= \frac{\rho \delta_d b U_j}{W} \frac{d}{dt} \left[tanh\left(\frac{\eta(t) - y_0}{b} \right) \right] - \frac{\rho}{2\alpha_{vc}^2} v_{ac}(t) abs(v_{ac}(t)). \end{aligned} \tag{8}$$

Here, the second term in the second equation corresponds to nonlinear losses at the labium due to vortex shedding [21], and α_{vc} is the corresponding *vena contracta* factor, estimated as 0.6 for the case of a sharp edge [22]. System (7)–(8) can be re-written as a system of $2m$ first-order neutral delay differential equations, with m the total number of modes taken into account (for more details on the calculations, see, for example, [20]). We investigate this system using a Matlab dedicated time-domain solver and the continuation toolbox DDE-Biftool [24, 23, 25], which has been adapted to allow for the continuation of equilibria and periodic solutions of NDDES, as well as their bifurcations in two parameters [26, 27, 20]. For numerical reasons, the time variables are rescaled with respect to the first resonance angular frequency ω_1.

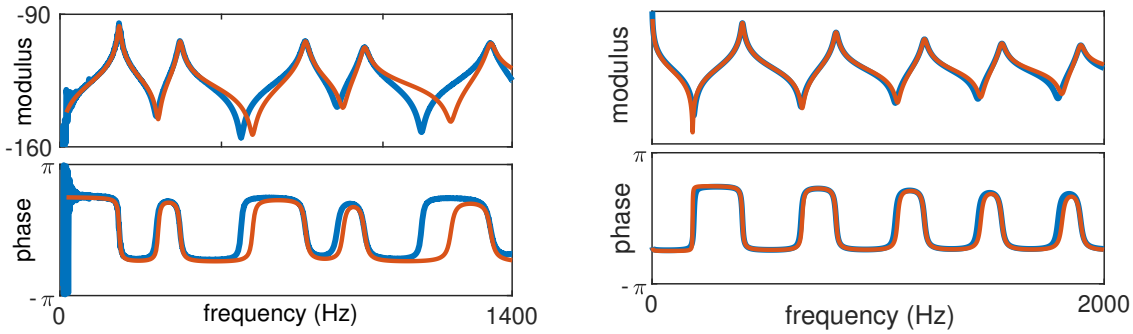

Figure 4: Modulus (top) and phase (bottom) of the admittance Y of a Chilean flute (left) and of an alto recorder (right). The experimentally measured admittance of the Chilean flute and the admittance determined analytically from the precise pipe geometry of the recorder are shown in blue. The corresponding fitted admittances written as a sum of resonance modes are shown in red.

3 Time-domain simulations

We now investigate the ability of the generic flute model (7)–(8) to reproduce the two qualitatively different non periodic sound regimes produced by the Chilean flute and the recorder. Although they have been shown recently to be both quasiperiodic [16], these two sound regimes show qualitative differences in terms of modulation frequency and spectral content. Compared to recorders, Chilean flutes produce deeply modulated sound regimes, with a low modulation frequency and a very rich spectrum with high energy levels in the higher order partials [28].

Here we perform time-domain simulations of system (7)–(8), considering two different sets of parameters corresponding to the recorder and the Chilean flute, respectively. The simulations are performed using the Matlab solver ddensd dedicated to neutral delay differential equations [42]. The resonator parameters are as discussed above (see Table 1) and the exciter parameters are mostly identical in both cases, except for the air jet length W. This is justified by the fact that this is fixed to $W = 4.25$ mm at the making stage for the recorder while it is a control parameter for the Chilean flute. For the similar case of transverse flutes, it has been estimated experimentally that the ratio W/h varies between 3 and 12 [29], and we consider here a (fixed) value of $W = 10$mm. The two sets of parameters are summarized in Table 2.

Figure 5 shows the simulated time series for both parameter sets, and for fixed values of the (rescaled) delay time $\tilde{\tau} = \omega_1 \tau$. Both simulated sound regimes show a modulation of the oscillation amplitude, which is reminiscent of the experimental time series (see Figure 1) [16]. The two sound regimes show qualitative differences in excellent agreement with the experimental observations. In particular, the modulation is deeper and the modulation frequency is much lower for the Chilean flute than for the recorder (note that different scales are used for the x-axis of the left and right panels in Figure 5). This is reminiscent of the strong beating component at a frequency close to 15Hz which has been shown to be characteristics of the sounds produced by these Chilean flutes [28, 15].

Figure 6 shows the Poincaré sections of both simulated time series, represented in a 3D-space whose dimensions are delayed version of the variable v_{ac}. More precisely, the embedding dimension is estimated (here as four) using a false nearest neighbor algorithm, and a suitable delay τ_e is selected by detecting the first zero of the auto-correlation of the signal $v_{ac}(t)$ [30]. The projected Poincaré sections are defined as the trajectory in the four-dimensional reconstructed phase space passing through a fixed value of $v_{ac}(t - 3\tau_e)$. In both cases, the Poincaré sections feature densely filled closed loop. It is worth noting that the seemingly self-intersections of the curve, observed in the case of the recorder (Figure 6, right), is only due to the further projection of the 3D picture onto a 2D plane by the printed Figure. Overall, this demonstrates the quasiperiodic nature of both simulated sounds.

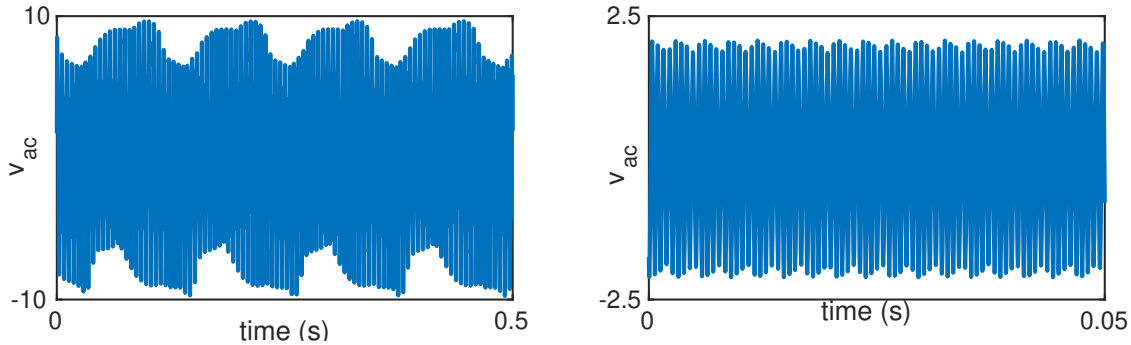

Figure 5: Simulated sound regimes: acoustical velocity v_{ac} with respect to time, for the Chilean flute (left) and recorder parameters (right). The rescaled delay time $\tilde{\tau}$ is 0.74 (left) and 0.295 (right), corresponding to pressure $P_m = 915$ Pa and $P_m = 4900$ Pa in the musician's mouth, respectively.

	a_0	b_0	c_0	a_1	ω_1	Q_1	a_2	ω_2	Q_2
Chilean flute	0	1.60	3.31	11.39	1157	26.07	7.04	2343	34.39
recorder	11.22	1.60	3.31	22.36	2510	44.9	16.39	5113	59.65
	a_3	ω_3	Q_3	a_4	ω_4	Q_4	a_5	ω_5	Q_5
Chilean flute	9.55	4796	50.67	8.12	5943	52.87	12.94	8419	58.00
recorder	12.64	7569	67.2	10.55	9719	73.57	10.32	11909	79.98

Table 1: Values of the modal parameter considered for the admittance of both the Chilean flute and the recorder.

Figures 7 and 8 show the modulus of the Fourier spectrum of the simulated acoustic velocity $v_{ac}(t)$ for both instruments. In each case, it allows to identify two *base frequencies* f_1 and f_2, such that f_1/f_2 is not rational and that all the peaks in the spectra appear at frequencies which are linear combinations of f_1 and f_2. Here, $f_1 \approx 188$ Hz and $f_2 \approx 367$ Hz for the Chilean flute, and $f_1 \approx 340$ Hz and $f_2 \approx 1558$ Hz for the recorder. Not only this confirms the quasiperiodicity of both simulated sound regimes, but also it allows for a more comprehensive comparison with the experimental data [16].

For the Chilean flute parameters, the simulated sound regime has a very rich spectrum, with high energy levels in the higher order partials [28], which is an important feature of the experimental sound regimes. Moreover, a similar analysis of the experimental sound regimes obtained with the particular Chilean flute whose measured admittance $Y(\omega)$ is considered here highlighted two base frequency of approximately 186Hz and 14Hz. This shows excellent agreement with the base frequency $f_1 \approx 188$Hz of the simulated sound and with the lowest modulation frequency $f_2 - f_1 \approx 8.6$Hz observed in the spectrum, which corresponds to the strong beating component at low frequency observed in the time series (Figure 5, left). For the recorder, the spectrum shows only a few numbers of well-identified peaks on the whole represented frequency range, and no peaks are observed below 100Hz. These differences in the spectral content are similar to the ones observed experimentally between the recorder and the Chilean flute sounds [28, 16]. Again, the base frequencies of the simulated sound are in good qualitative agreement with the base frequencies obtained on an experimentally recorded sound, which were close to 400Hz and to 1550Hz for a close (but not identical) configuration of the resonator [16].

Overall, these results demonstrate the ability of the generic model of flute-like instruments to reproduce the two qualitatively different quasiperiodic regimes produced by the two instruments considered in this article. In simulation, the exciter parameters were mostly identical for both the recorder and the Chilean flute. As such, the peculiar resonator geometry of Chilean flutes, which is accounted for through its measured input admittance $Y(\omega)$, seems to play a crucial role in the emergence, at low

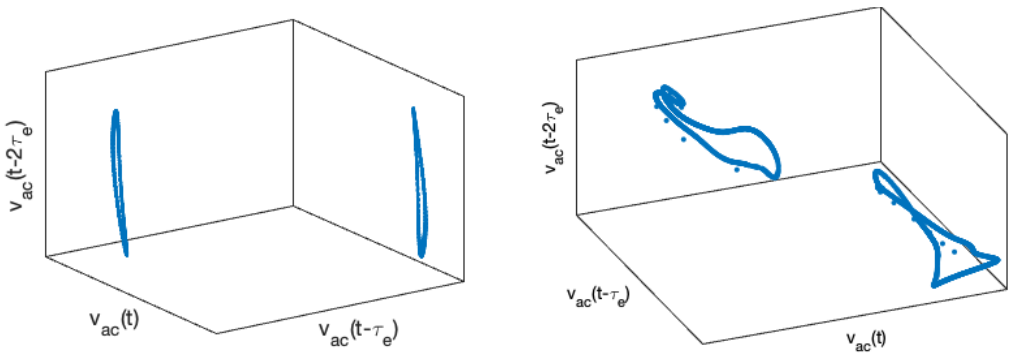

Figure 6: Projection of the Poincaré sections of the two simulated time series shown in Figure 5, for the Chilean flute parameters (left) and the recorder parameters (right), and for a rescaled delay $\tilde{\tau} = 0.74$ (left) and $\tilde{\tau}$ =0.295 (right). The delay τ_e is estimated at thefirst zero of the autocorrelation of $v_{ac}(t)$.

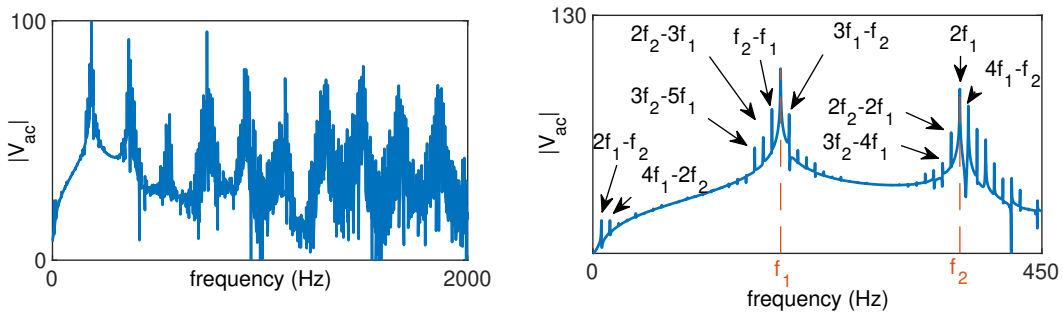

Figure 7: Modulus of the spectrum (log scale) of the simulated time series shown in Figure 5 (left), for the Chilean flute parameters and for a dimensionless delay of $\omega_1\tau = 0.74$. The right panel shows an enlargement of the spectrum shown in the left panel over a low frequency range. Shown are the two *base frequencies* f_1 and f_2 of the quasiperiodic regime, as well as some of their linear combinations.

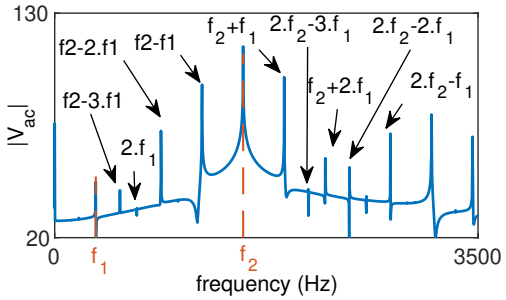

Figure 8: Modulus of the spectrum (log scale) of the simulated time series shown in Figure 5 (right), for the recorder parameters and for a dimensionless delay of $\omega_1\tau = 0.295$. Shown are the two *base frequencies* f_1 and f_2 of the quasiperiodic regime, as well as some of their linear combinations.

	h	W	y_0	ρ	α_{vc}
Chilean flute	10^{-3}	10^{-2}	$2 \cdot 10^{-4}$	1.2	0.6
recorder	10^{-3}	$4.25 \cdot 10^{-3}$	10^{-4}	1.2	0.6

Table 2: Values of the parameters associated with the exciter, for both the Chilean flute and the recorder.

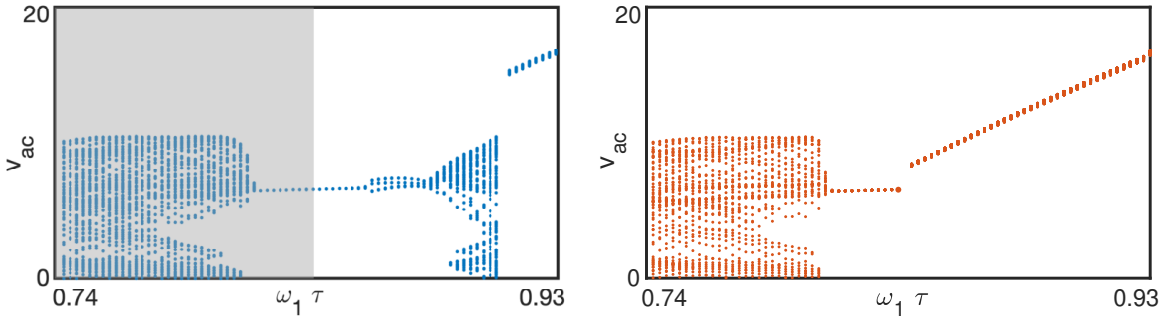

Figure 9: One-parameter bifurcation diagram representing the local maxima of the simulated acoustic velocity v_{ac} with respect to the delay time $\tilde{\tau}$, for an increasing (left) and a decreasing (right) delay $\tilde{\tau}$. The shaded area indicates the parameter range of the spectrogram in Figure 10.

values of the mouth pressure, of a stable quasiperiodic regime with a strong, low-frequency beating component and a rich spectrum.

4 Numerical bifurcation analysis

We now focus on the case of the Chilean flute, and explore the influence of two parameters of practical importance on the existence and stability of the quasiperiodic regime discussed in the previous section. The influence of $\tilde{\tau}$, which is (indirectly) the main control parameter of the musician, is explored in time-domain simulations and through a bifurcation analysis performed with the continuation toolbox DDE-Biftool. Secondly, we investigate the influence of the inharmonicity (as defined in the introduction) which is related to the geometry of the resonator and is, as such, of particular importance in the context of instrument making [33, 34].

4.1 Influence of the delay $\tilde{\tau}$

Figure 9 shows a one-parameter bifurcation diagram obtained from time-domain simulation for the Chilean flute parameters. It represents the local maxima of the acoustic velocity $v_{ac}(t)$ for an increasing and decreasing value of $\tilde{\tau}$ (corresponding to a decreasing and increasing pressure in the musician's mouth, respectively). The starting value $\tilde{\tau} = 0.74$ corresponds to the delay time considered in Figures 5-7. For each value of $\tilde{\tau}$, the initial conditions over the history interval $[-\tilde{\tau} + t_0, t_0]$ are set to the previously calculated solution, *i.e.* for a slightly smaller (respectively, larger) $\tilde{\tau}$. This shows that, when increasing the delay, the system remains on the quasiperiodic regime shown in Figure 5 up to $\tilde{\tau} = 0.82$. However, the modulation which was clearly visible in Figure 5 becomes less and less deep. From $\tilde{\tau} = 0.82$, a periodic solution is observed, which corresponds, in Figure 9 (left), to a fixed number of (constant) maxima of v_{ac} for each value of $\tilde{\tau}$. Increasing $\tilde{\tau}$ further leads to the emergence of another quasiperiodic regime around $\tilde{\tau} = 0.88$. It exists only on a small range of $\tilde{\tau}$ and the system subsequently jumps, at $\tilde{\tau}$=0.9, towards another periodic regime whose amplitude increases with the delay. Starting from this periodic regime and decreasing the delay $\tilde{\tau}$ back down to 0.74 (Figure 9, right), one observes a hysteresis

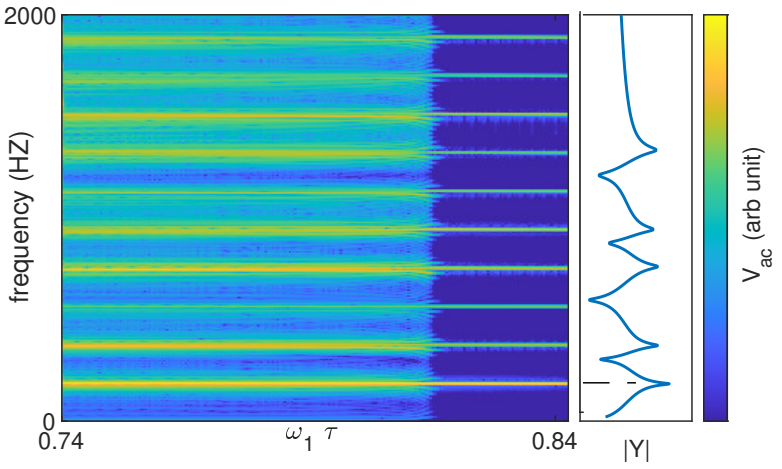

Figure 10: Left: Spectrogram of the simulated acoustic velocity v_{ac} shown in Figure 9 (left, shaded area), for a increasing value of the delay $\tilde{\tau}$. Right: modulus of the fitted input admittance $Y(\omega)$ of the Chilean flute, already shown in Figure 4 (top, left).

phenomenon. In particular, the quasiperiodic regime observed around $\tilde{\tau}$= 0.88 when $\tilde{\tau}$ is increased is not observed for a decreasing $\tilde{\tau}$. Rather, the system remains on the same branch of periodic solutions down to $\tilde{\tau} = 0.835$, where it jumps back to another periodic regime which was already observed when increasing $\tilde{\tau}$. Decreasing the delay further leads to the emergence of the quasiperiodic regime highlighted in the previous section, without hysteresis effect compared to the case where the delay is increased.

Figure 10 shows the spectrogram of the acoustic velocity v_{ac} around the transition between the quasiperiodic and the periodic regime, observed when $\tilde{\tau}$ is increased from 0.74 to 0.84. This parameter range is highlighted by a shaded area in Figure 9 (left). In Figure 10, the x-axis is $\tilde{\tau}$, the y-axis is the frequency and the modulus of the Fourier spectrum at each frequency is represented by the color scale. The right panel reproduces the modulus of the fitted input admittance $Y(\omega)$ of the Chilean flute, to allow for a comparison between the spectral content of the simulated acoustic velocity v_{ac} and the resonance frequencies of the passive system. This shows that the system undergoes a transition from the quasiperiodic sound regime towards the first register, that is to say a periodic regime whose frequency is very close to the first resonance frequency. These results suggest that the quasiperiodic regime emerges from a torus bifurcation of the first register. In comparison, for the case of transverse flutes or recorders, the destabilisation of the first register occurring when τ is decreased (i.e. when the mouth pressure is increased) classically leads to a transition towards another register, that is to say towards a stable periodic regime whose frequency is close to one of the upper order resonance frequencies [32, 31, 35].

This dynamics is investigated further by performing a bifurcation analysis using advanced numerical continuation methods. Figure 11 shows the one-parameter bifurcation diagram of system (7)–(8) in the dimensionless delay $\tilde{\tau}$. Periodic solutions are represented by the maximum value of the acoustic velocity $v_{ac}(t)$ (left panel) and by their frequency (right panel). For a decreasing $\tilde{\tau}$ (which corresponds to an increasing pressure in the musician's mouth), successive periodic solution branches emerge in successive Hopf bifurcations H. The right panel in Figure 11 shows that each branch of periodic solutions corresponds to a particular register of the instrument, and that these registers appear in increasing order (and thus with increasing oscillation frequency) when decreasing $\tilde{\tau}$. Figure 11 shows that all periodic solutions branches are unstable immediately after they emerge in a Hopf bifurcation.

The third, fourth and fifth register stabilise successively in torus bifurcations encountered when the delay $\tilde{\tau}$ is decreased, and they remain stable down to the minimal considered value of $\tilde{\tau}$. On the contrary, the first and second registers stabilise and destabilise several times through torus bifurcations T but also,

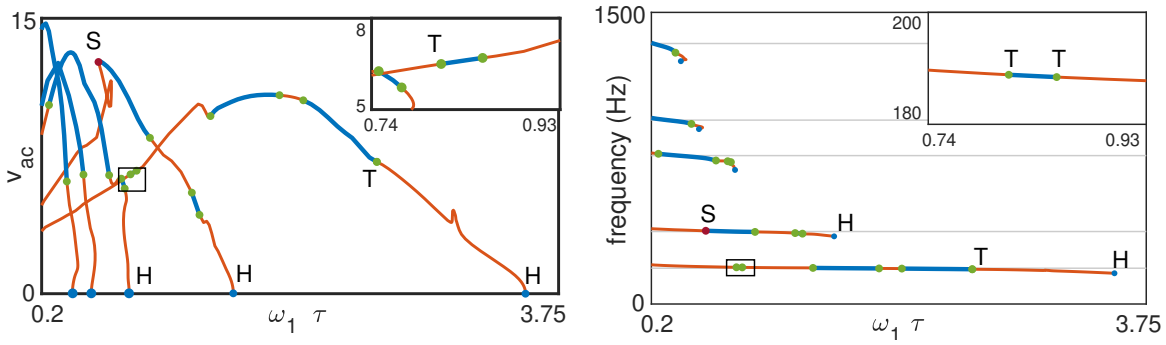

Figure 11: One-parameter bifurcation diagram of (7)–(8) in the dimensionless delay $\tilde{\tau}$, showing the maximum amplitude of the acoustic velocity v_{ac} (left) and the frequency (right) along branches of periodic solutions. The stable and unstable solutions are represented in blue and red, respectively. Shown are Hopf bifurcation points H (blue dots), torus bifurcation points T (green dots) and point S of saddle-node bifurcation of periodic orbits (red dot). In the right panel, the light gray lines show the resonance frequencies of the instrument. The insets show enlargements of the branch of periodic solution corresponding to the first register on the range of $\tilde{\tau}$ represented in Figure 9.

for the second register, in a saddle-node bifurcation of periodic orbits S. The first register displays three successive stability ranges. In particular, a small range of stability is observed for $0.81 < \tilde{\tau} < 0.85$. On this range of $\tilde{\tau}$, the second register is also stable. This multistability explains the hysteresis phenomenon observed in simulation in Figure 9. Moreover, the change of stability of the first register at $\tilde{\tau} = 0.82$ corresponds to the value at which the transition between a stable quasiperiodic regime and the first register is observed in simulation (see Figures 9 and 10).

Overall, as $\tilde{\tau}$ is decreased, an increasing level of multistability is observed between the higher-order registers. More precisely, and as already discussed in the literature [31, 32, 20], the lower order registers (with the lower oscillation frequencies, thus corresponding to the lower pitch notes) emerge, stabilise and subsequently destabilise for larger values of τ (i.e. for smaller mouth pressure) than the higher order registers. This corresponds to the experimental observations, where successive notes with higher and higher pitch are obtained when the musician blows harder and harder into the instrument [31, 35].

4.2 Influence of the detuning

The inharmonicity is defined, in the musical context, as the detuning between the upper order resonance frequencies and the integer multiples of the first resonance frequency. Here we investigate its influence on the bifurcation scenario detailed in Figure 11. This parameter depends on the details of the internal geometry of the instrument. It is therefore adjusted at the making stage, and it is of particular importance from the instrument maker's point of view: not only are the values of the resonance frequencies related directly to the intonation of the instrument, but different studies have also shown that, on clarinet-like instruments, a strong inharmonicity can favor the emergence of stable non-periodic sound regimes [34, 36].

The specific shape of the Chilean flute resonator results in a strong inharmonicity, as already shown in Figure 4. Compared to the input admittance of the recorder, where resonance peaks appear at frequencies close to integer multiples of the first resonance frequency, the input admittance of the Chilean flute rather shows a series of double resonance peaks. Using a theoretical model of the resonator, Blanc *et al* [15] showed that the fact that the instrument is made of two cylinders of different radius, with one open and one close end, results in an admittance showing series of double resonance peaks. More precisely, one finds pairs of resonance peaks which are located on both sides of the theoretical resonance frequencies of a close-open cylindrical pipe of half the total length of the instrument. The space between two consecutive peaks depends on the ratio between the radius of the two cylindrical

parts of the resonator.

To investigate the influence of this specific feature of the admittance of Chilean flutes on the emergence of a stable, deeply modulated quasiperiodic regime, we define a *global* inharmonicity parameter Γ, which allows to change the input admittance of the instrument in a continuous manner from a perfectly harmonic case (when $\Gamma = 0$) to the case of the Chilean flute measured admittance (Figure 4), when $\Gamma = 1$. More precisely, we define, for each resonance mode, a parameter ξ_n characterising the inharmonicity of the nth resonance mode as measured for the considered Chilean flute:

$$\xi_n = \frac{\omega_n}{(2n-1)\omega_1} - 1. \tag{9}$$

From there, one can investigate the influence of the inharmonicity by changing Γ and by defining the resonance (angular) frequencies of the instrument as follows:

$$\omega_{\Gamma n} = (1 + \Gamma\xi_n)(2n-1)\omega_1. \tag{10}$$

It is straightforward from equation (10) that, for $\Gamma = 0$, one has$f_n = (2n-1)f_1$ which corresponds to the ideal case of a perfectly harmonic cylindrical resonator with one open and one close end. On the other hand, for $\Gamma = 1$, one gets the resonance frequencies ω_n measured on the actual Chilean flute, and given in Table 1. Because the Chilean flute has a negative inharmonicity (*i.e.* the resonance frequencies are shifted towards lower frequencies compared to the perfectly harmonic case), a positive (negative) Γ corresponds here to a negative (positive) inharmonicity.

Figure 12 shows the bifurcation diagram of system (7)–(8) in the $(\tilde{\tau}, \Gamma)$-plane of rescaled delay and inharmonicity parameter. Shown are the curves H of Hopf bifurcations at which the different registers (whose range are indicated by numbers) emerge. Figure 12 shows that changing Γ has little effect on the threshold, in $\tilde{\tau}$, at which the first register emerges. Its influence is more important for the upper order registers. In particular, going from a strong negative inharmonicity (large positive value of Γ) towards a positive inharmonicity ($\Gamma < 0$) leads to a decrease in the value of $\tilde{\tau}$ at which the second register emerges. From a musical point of view, this means that the pressure in the musician mouth needs to be much higher in the latter case to reach the second register. As such, this note will be much more difficult to play. Interestingly, the second and the fourth register completely disappear for an important negative inharmonicity (close to $\Gamma = 2$).

The inset in Figure 12 provides details on the influence of Γ on the emergence of the stable quasiperiodic regime highlighted in Figure 9. Shown are two torus bifurcation curves T, corresponding to the successive stabilisation and destabilisation of the first register, observed for the smaller value of $\tilde{\tau}$ in Figure 11. As such, in the inset in Figure 12, the leftmost curve T corresponds to the threshold at which the quasiperiodic regime observed in time-domain simulation emerges (see Figure 9). The inset in Figure 12 also shows a curve S of saddle-node bifurcation of periodic orbits and curves PD of period doubling bifurcations. The curve S displays several cusps and two 1:1 resonance points, each of whom corresponding to a connection between the curve S and one of the two curves T [17]. The curves PD of period doubling bifurcations connect to the rightmost curve T at 1:2 resonances points [17]. Overall, the results in Figure 12 show that, when decreasing Γ from 1 (*i.e.* for a weaker negative inharmonicity compared to the Chilean flute) the value of $\tilde{\tau}$ for which the destabilising (i.e. leftmost) torus bifurcation is observed first decreases and subsequently increases when Γ is decreased from 0.85. More importantly, none of the represented bifurcations is observed below $\Gamma = 0.58$: as the inset in Figure 12 shows, below this value, the last sequence of stabilisation - destabilisation of the first register, which was observed when decreasing $\tilde{\tau}$ (see Figure 11), is not observed anymore. One thus expects that the stable quasiperiodic regime described above is not observed anymore when starting from the first register and decreasing the delay $\tilde{\tau}$, when $\Gamma < 0.58$. Overall, these results highlight the strong influence of inharmonicity on the emergence of both stable periodic and quasiperiodic sound regimes.

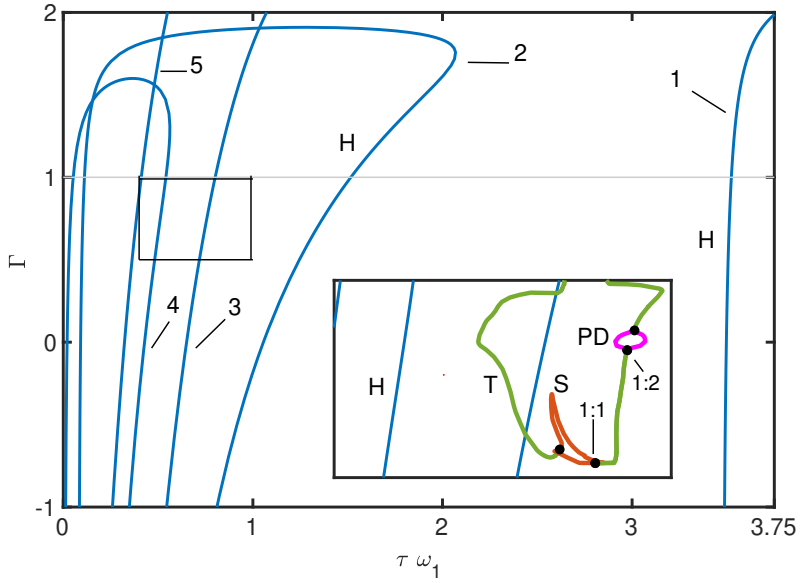

Figure 12: Two-parameter bifurcation diagram of (7)–(8) in the dimensionless delay $\tilde{\tau}$ and the inharmonicity parameter Γ. Shown are the Hopf bifurcation curves H (blue), and numbers indicate the register emerging at each Hopf bifurcation curve. The horizontal grey line at $\Gamma = 1$ highlights the inharmonicity corresponding to the case of the Chilean flute. The inset shows an enlargement of the bifurcation diagram in the framed parameter region, showing curves T of torus bifurcation (green), curve S of saddle-node bifurcation of periodic solutions (brown) and curves PD of period doubling bifurcations (pink). The black dots highlight 1:1 and 1:2 resonances.

5 Conclusion

The recorder and the prehispanic Chilean flute considered in the article are very different, despite a common sound production mechanism. The generic model of flute-like instruments, written as a system of NDDEs, is able to reproduce convincing quasiperiodic sound regimes: for each instrument, important properties of these regime are qualitatively comparable with those of experimentally-recorded sounds. This includes the spectral content and the amplitude and frequency of the observed modulation in time series.

The process through which quasiperiodic sounds emerge has been highlighted by performing a numerical bifurcation analysis. A stable quasiperiodic regime emerges from the destabilisation of the first register in a torus bifurcation when the blowing pressure in increased, and is observed over a range of delay time (blowing pressure) values. The detuning between the different acoustic resonance frequencies of the air column inside the instrument proved to be a key parameter to control the emergence of quasiperiodic regimes. In particular, decreasing the inharmonicity can lead to a qualitatively different bifurcation scenarios, where the stable quasiperiodic regime is not observed anymore. Similarly, some registers of the instrument (*i.e.* some notes of the musical scale) can entirely disappear for a strong positive inharmonicity. Finally, our bifurcation analysis unveils that not only the inharmonicity plays a key role, but also that positive and negative inharmonicity leads to qualitatively different bifurcation scenario when the mouth pressure is varied. Since there is a direct link between the geometry of the flute and the value of the detuning parameter, our results suggest that the particular shape of the prehispanic Chilean flute may be inspired by the will of makers to favor quasiperiodic regimes.

From a more general point of view, our study demonstrates that the numerical tools dedicated to the continuation of periodic solutions of NDDEs and their bifurcations allow to investigate the dynamics of complicated systems originating from actual experiments and applications. We expect that this might be of general interest, beyond the case of acoustics applications.

Acknowledgments

This work is supported by CONICYT through FONDECYT Project No. 1201551.

References

[1] M. E. McIntyre, R. T. Schumacher and J. Woodhouse, On the oscillations of musical instruments, *The Journal of the Acoustical Society of America*, **74** (1983), 1325–1345

[2] B. Fabre, J. Gilbert and A. Hirschberg, Modeling of wind instruments, in *Springer Handbook of Systematic Musicology* (ed. R. Bader), Springer, Berlin, Heidelberg, (2018), 121–139.

[3] A. Chaigne and J. Kergomard, *Acoustics of musical instruments*, Springer New York, 2016.

[4] B. Fabre and A. Hirschberg, Physical modeling of flue instruments: A review of lumped models, *Acta Acustica united with Acustica*, **86** (2000), 599–610.

[5] A. W. Nolle, Sinuous instability of a planar air jet: Propagation parameters and acoustic excitation, *The Journal of the Acoustical Society of America*, **103** (1998), 3690–3705.

[6] M. P. Verge, B. Fabre, W. E. A. Mahu, A. Hirschberg, R. R. van Hassel, A. P. J. Wijnands, J. J. de Vries, and C. J. Hogendoorn Jet formation and jet velocity fluctuations in a flue organ pipe, *The Journal of the Acoustical Society of America*, **95** (1994), 1119–1132.

[7] P. G. Drazin, *Introduction to hydrodynamic stability*, Cambridge university press, 2002.

[8] P. de la Cuadra, *The sound of oscillating air jets: Physics, modeling and simulation in flute-like instruments*, Ph.D thesis, Stanford University, 2006.

[9] P. de la Cuadra, C. Vergez and B. Fabre, Visualization and analysis of jet oscillation under transverse acoustic perturbation, *Journal of Flow Visualization and Image Processing*, **14** (2007).

[10] M. P. Verge, *Aeroacoustics of confined jets: with applications to the physical modeling of recorder-like instruments*, Ph.D thesis, Technische Universiteit Eindhoven, 1995.

[11] F. Blanc, V. François, B. Fabre, P. de la Cuadra and P.-Y. Lagrée, Modeling the receptivity of an air jet to transverse acoustic disturbance with application to musical instruments, *The Journal of the Acoustical Society of America*, **135** (2014), 3221–3230.

[12] J.-P. Dalmont, Acoustic impedance measurement, Part I: A review, *Journal of Sound and Vibration*, **243** (2001), 427–439.

[13] J.-P. Dalmont, Acoustic impedance measurement, Part II: A new calibration method, *Journal of Sound and Vibration*, **243** (2001), 441–459.

[14] P.-A. Taillard, F. Silva, P. Guillemain and J. Kergomard, Modal analysis of the input impedance of wind instruments. Application to the sound synthesis of a clarinet, *Applied acoustics*, **141** (2018), 271–280.

[15] F. Blanc, P. de la Cuadra, B. Fabre, G. Castillo and C. Vergez, Acoustics of the *flautas de chinos*, in *Proceeding of 20th International Symposium on Music Acoustics*, (2010).

[16] S. Terrien, C. Vergez, P. de la Cuadra and B. Fabre, Experimental analysis of non-periodic sound regimes in flute-like musical instruments, *The Journal of the Acoustical Society of America*, **149** (2021), 2100–2108.

[17] Y. A. Kuznetsov, *Elements of applied bifurcation theory*, Springer, **112** (2013), 2100–2108.

[18] A. Lefebvre, G. Goudou and G. Scavone, The Wind Instrument Acoustic Toolkit, Available from: http://www.music.mcgill.ca/caml/wiat/.

[19] D. H. Lyons, Resonance frequencies of the recorder (English flute), *The Journal of the Acoustical Society of America*, **70** (1981), 1239–1247.

[20] S. Terrien, C. Vergez, B. Fabre and D. A. W. Barton, Calculation of the steady-state oscillations of a flute model using the orthogonal collocation method, *Acta Acustica united with Acustica*, **100** (2014), 690–704.

[21] B. Fabre, A. Hirschberg, A. P. J. Wijnands, Vortex shedding in steady oscillation of a flue organ pipe, *Acta Acustica united with Acustica*, **82** (1996), 863–877.

[22] G. Falkovich, *Fluid mechanics: A short course for physicists*, Cambridge university press, 2011.

[23] K. Engelborghs, T. Luzyanina, and D. Roose, Numerical bifurcation analysis of delay differential equations using DDE-BIFTOOL, *ACM Trans. Math. Softw.*, **28** (2002), 1–21.

[24] K. Engelborghs, T. Luzyanina, and G. Samaey, DDE-BIFTOOL v. 2.00: a Matlab package for bifurcation analysis of delay differential equations, Technical Report TW-330, Department of Computer Science, K.U. Leuven, Belgium, 2001.

[25] J. Sieber, K. Engelborghs, T. Luzyanina, G. Samaey, D. Roose, Manual - Bifurcation analysis of delay differential equations, Available from: arxiv.org/abs/1406.7144.

[26] D. A. W. Barton, B. Krauskopf and R. E. Wilson, Collocation schemes for periodic solutions of neutral delay differential equations, *Journal of Difference Equations and Applications*, **12** (2006), 1087–1101.

[27] D. A. W. Barton, B. Krauskopf and R. E. Wilson, Bifurcation analysis tools for neutral delay equations: a case study, *IFAC Proceedings Volumes*, **39** (2006), 36–41.

[28] H. Wright, and D. Campbell, Analysis of the sound of chilean pifilca flutes, *The Galpin Society Journal*, **51** (1998), 51–63.

[29] C. Vauthrin, B. Fabre and I. Cossette, How does a flute player adapt his breathing and playing to musical tasks?, *Acta Acustica united with Acustica*, **101** (2015), 224–237.

[30] H. Abarbanel, *Analysis of observed chaotic data*, Springer, 2012.

[31] R. Auvray, B. Fabre and P.-Y. Lagrée, Regime change and oscillation thresholds in recorder-like instruments, *The Journal of the Acoustical Society of America*, **131** (2012), 1574–1585.

[32] S. Terrien, C. Vergez and B. Fabre, Flute-like musical instruments: a toy model investigated through numerical continuation, *Journal of Sound and Vibration*, **332** (2013), 3833–3848.

[33] J.-P. Dalmont, B. Gazengel, J. Gilbert and J. Kergomard, Some aspects of tuning and clean intonation in reed instruments, *Applied Acoustics*, **46** (1995), 19–60.

[34] J.-B. Doc and C. Vergez, Oscillation regimes produced by an alto saxophone: Influence of the control parameters and the bore inharmonicity, *The Journal of the Acoustical Society of America*, **137** (2015), 1756–1765.

[35] S. Terrien, R. Blandin, C. Vergez and B. Fabre, Regime change thresholds in recorder-like instruments: Influence of the mouth pressure dynamics, *Acta Acustica united with Acustica*, **101** (2015), 300–316.

[36] J.-B. Doc, C. Vergez and S. Missoum, A minimal model of a single-reed instrument producing quasi-periodic sounds, *Acta Acustica united with Acustica*, **100** (2014), 543–554.

[37] K. Engelborghs and D. Roose, Smoothness loss of periodic solutions of a neutral functional-differential equation: on a bifurcation of the essential spectrum, *Dynamics and Stability of Systems*, **14** (1999), 255–273.

[38] C. Maganza, R. Caussé and F. Laloë, Bifurcations, period doublings and chaos in clarinetlike systems, *Europhysics Letters*, **1** (1986), 295.

[39] N.H. Fletcher, Nonlinear dynamics and chaos in musical instruments, *Complexity International*, **1** (1994), 106–117.

[40] J.K. Hale and S.M.V. Lunel, *Introduction to functional differential equations*, Springer, 2013.

[41] O. Diekmann, S.A. Van Gils, S. M. Lunel and H. O. Walther, *Delay equations: functional-, complex-, and nonlinear analysis*, Springer, 2012.

[42] L.F. Shampine, Dissipative approximations to neutral DDEs, *Applied Mathematics and Computation*, **203**(2) (2008), 641–648.

[43] J. Gilbert, S. Maugeais, and C. Vergez, Minimal blowing pressure allowing periodic oscillations in a simplified reed musical instrument model: Bouasse-Benade prescription assessed through numerical continuation, *Acta Acustica*, **4**(6) (2020), 27.

[44] D. Roose and R. Szalai, Continuation and bifurcation analysis of delay differential equations, in *Numerical continuation methods for dynamical systems* (Eds. B. Krauskopf, H.M. Osinga and J. Galán-Vioque), Springer, Dordrecht, 2007. 359-399.